



An Integrated Convolutional Neural Networks and Light Gradient Boosting Approach for Flood Classification Using Sentinel-1 SAR Satellite Imagery

Siddiq Ahmad Anshori¹, Asep Id Hadiana², Fatan Kasyidi³

^{1,2,3}Department of Informatics, Universitas Jenderal Achmad Yani, Cimahi 40531, Indonesia

¹siddiq.anshori@gmail.com, ²asep.hadiana@lecture.unjani.ac.id, ³fatan.kasyidi@lecture.unjani.ac.id

ARTICLE INFORMATION

Article History:

Received: December 10, 2024

Last Revision: April 21, 2025

Published Online: April 30, 2025

KEYWORDS

Flood Classification,
Sentinel-1 SAR Imagery,
CNN-ResNet50,
LightGBM,
Disaster Management

CORRESPONDENCE

Phone: 085659425705

E-mail: siddiq.anshori@gmail.com

ABSTRACT

Flood classification plays a crucial role in disaster mitigation, particularly in areas frequently affected by floods. This study proposes a novel model combining Convolutional Neural Networks (CNN) using ResNet-50 and Light Gradient Boosting Machine (LightGBM) for classifying flood and non-flood areas using Sentinel-1 SAR imagery. The dataset used consists of 21,016 images, evenly distributed between flood and non-flood classes, and processed through resizing, normalization, denoising, and augmentation. Feature extraction was conducted using the ResNet-50 architecture, which captured spatial and textural patterns efficiently, followed by LightGBM for classification. The proposed model achieved a high accuracy of 96%, with Precision, Recall, and F1-scores exceeding 95% for both classes. The evaluation metrics, including Precision-Recall Curve with an AUC of 0.9852 and a Confusion Matrix, confirmed the model's robustness and balance in classifying both categories. Additionally, comparisons with previous research, such as SAR-FloodNet, demonstrated the superiority of the proposed approach, achieving a 2% improvement in accuracy. Despite these results, limitations such as the exclusive use of Sentinel-1 data and the lack of validation across diverse environmental conditions remain. Future research should explore integrating multispectral Sentinel-2 data and testing on broader datasets to enhance scalability and reliability. The findings underscore the model's potential for real-world applications in flood monitoring and disaster management systems.

1. INTRODUCTION

Floods are among the most destructive natural disasters, particularly in densely populated areas, low-lying topographies, and regions with extreme rainfall. The impacts of this disaster include infrastructure damage, loss of housing, and even casualties [1]. Over recent decades, climate change has intensified flood risks through increased rainfall intensity and rising sea levels [2], [3]. Studies show that floods are the most frequent hydro-meteorological hazards, causing global economic losses of approximately \$10 billion annually. The United Nations University estimates that over half a billion people are affected by floods each year, and this figure could rise to two billion by 2050 due to ongoing climate change and rapid urbanization [4]. Hence, innovative approaches are required to improve flood classification and reduce its impacts, especially through the integration of remote

sensing technologies and machine learning into early warning systems [4].

Remote sensing using satellite imagery has become a crucial tool in flood disaster monitoring and management. One of the most utilized data sources is Synthetic Aperture Radar (SAR) imagery from Sentinel-1 satellites, part of the Copernicus program by the European Space Agency (ESA). SAR is effective for flood monitoring, even in data-scarce or cloud-covered regions [5], [6]. Its advantage lies in its ability to penetrate clouds and operate regardless of lighting conditions. Sentinel-1, operating in VV (Vertical-Vertical) and VH (Vertical-Horizontal) polarization modes, provides high-resolution imagery (up to 5 m × 20 m), making it suitable for large-scale flood mapping [7]. By combining satellite data and machine learning, we can develop faster, more accurate flood classification models

to support government response and community resilience efforts [8].

Machine learning (ML) provides powerful methods to analyze large-scale datasets such as satellite imagery. Deep learning, a subset of ML, leverages Artificial Neural Networks (ANNs) to achieve high accuracy and solve complex problems by learning from data patterns. Prior studies have shown that deep learning significantly enhances satellite image classification tasks [9]. One of the most used algorithms in this field is the Convolutional Neural Network (CNN), which extracts essential features from grid-structured data like 2D images. CNNs are particularly effective in object classification, including flood detection using radar imagery [10].

Nevertheless, challenges persist in handling high-dimensional and imbalanced datasets. Ensemble learning offers an effective solution by combining predictions from multiple models to improve classification performance and reduce overfitting, bias, or variance [11], [12]. There are two main approaches in ensemble learning: bagging (bootstrap aggregating), which reduces variance by training models in parallel, and boosting, which improves prediction accuracy by sequentially correcting previous model errors [13]. Boosting techniques are highly popular due to their ability to iteratively improve accuracy, especially on complex data. One of the most efficient boosting implementations is Gradient Boosting, which builds decision trees iteratively to correct prior errors [14]. However, this method can be computationally expensive when applied to large datasets. To address this, Light Gradient Boosting Machine (LightGBM) was introduced to improve training speed and memory efficiency without sacrificing accuracy.

LightGBM, a gradient boosting framework, introduces key optimizations such as Gradient-based One-Side Sampling (GOSS) and Exclusive Feature Bundling (EFB). GOSS prioritizes training on samples with large gradients, focusing on those contributing most to errors. EFB, meanwhile, reduces data dimensionality by grouping mutually exclusive features, helping maintain performance on high-dimensional data [14], [15]. These innovations make LightGBM suitable for handling class imbalance, overfitting, and high-dimensional features common challenges in satellite image classification tasks [16].

The main objective of this study is to design and evaluate a robust computational model for classifying flood events using Sentinel-1 satellite radar imagery. This research integrates Convolutional Neural Network (CNN) for deep feature extraction and Light Gradient Boosting Machine (LightGBM) for classification, forming a hybrid approach tailored to the challenges of satellite image analysis. Specifically, the model aims to accurately distinguish between 'Flood' and 'Non-Flood' regions within high-resolution SAR imagery. This methodological combination is intended to overcome the limitations of earlier models such as SAR-FloodNet [17], which, although effective, utilized a patch-based architecture that struggled to generalize across the diverse image samples found in datasets like SEN12-FLOOD. By leveraging CNN's capability to extract spatial features and LightGBM's efficiency in handling high-dimensional data and class imbalance, the proposed model seeks to achieve better performance, increased generalization ability,

reduced training complexity, and improved classification stability across heterogeneous and large-scale datasets.

This research presents several key contributions beyond previous studies. First, it introduces a hybrid classification model that combines CNN-ResNet50 for feature extraction with LightGBM for final classification. This approach is designed to improve efficiency and accuracy when handling large and diverse datasets, such as SEN12-FLOOD, compared to the patch-based method utilized in SAR-FloodNet [17]. Second, the study applies a targeted data augmentation strategy to address class imbalance an aspect often overlooked in prior works. The proposed model achieved a classification accuracy of 96%, outperforming SAR-FloodNet's 94% [17], thereby validating the effectiveness of this integrated method. Lastly, this study emphasizes the potential for incorporating multispectral data sources, such as Sentinel-2, in future work, which could offer complementary information and enhance flood detection capabilities.

2. RELATED WORK

Sentinel-1, which utilizes Synthetic Aperture Radar (SAR) technology, has proven to be an effective data source for flood classification. Its ability to capture imagery under adverse weather conditions or darkness makes it particularly valuable. Several previous studies have demonstrated the effectiveness of Sentinel-1 in identifying flood-affected areas, especially in challenging weather using multi-temporal SAR data, with results showing high classification accuracy [18], [19]. Moreover, this capability makes Sentinel-1 a strong foundation for developing robust flood classification models across various environmental conditions.

Building upon this, recent research has explored the integration of machine learning with geospatial data analysis to model flood hazards. These studies emphasize the importance of combining SAR Sentinel-1 with other geospatial data sources to enhance flood prediction and risk assessment [20]. For example, a study in Punjab, Pakistan, demonstrated the effectiveness of integrating remote sensing data with machine learning models to produce accurate flood susceptibility maps, offering valuable insights for disaster management and mitigation planning [21]. Similarly, previous studies have also utilized Sentinel-1 imagery to monitor flood disasters in agricultural areas in Indonesia, further supporting its strength in identifying standing water [6]. Despite these advantages, SAR image processing presents technical challenges, particularly due to speckle noise, which can reduce classification accuracy if not addressed properly.

To address such challenges in feature representation and classification accuracy, deep learning especially Convolutional Neural Networks (CNNs) has emerged as a powerful tool for satellite imagery analysis. CNNs are known for their capability in feature extraction and classification, particularly with complex spatial data such as SAR imagery. For instance, the SAR-FloodNet CNN model was developed to classify floods in Sentinel-1 SAR imagery and demonstrated high accuracy, although limitations remained in its ability to generalize across large and diverse datasets [17]. CNN-based models have also been successfully applied to multi-temporal imagery to

detect changes in surface conditions caused by flooding, leveraging CNN's strength in capturing spatial patterns [19].

However, despite its success, the CNN approach often encounters obstacles such as long training times and overfitting risks, particularly when working with limited datasets. Several studies have attempted to mitigate these challenges by employing deeper CNN architectures. While deeper networks can enhance feature representation, they may compromise computational efficiency and struggle with generalization on large-scale datasets [22]. To overcome the limitations of traditional CNNs, researchers have explored advanced architectures like ResNet-50. For example, prior studies modified ResNet-50 with a multi-scale attention mechanism to improve recognition accuracy, illustrating the model's strength in capturing more complex and abstract features. [23]. ResNet-50, with residual learning and a deeper architecture, has proven to outperform traditional CNN models in various classification tasks. However, this study did not combine ResNet-50 with ensemble learning methods such as LightGBM, which can improve classification efficiency and accuracy [23].

Other studies have shown that ResNet-50, with its ability to handle deeper networks and reduce the vanishing gradient problem, achieves higher classification accuracy compared to traditional CNN models, especially when working with large and complex datasets [24]. The main advantage of ResNet-50 lies in its ability to handle more complex and deeper features, thus improving classification accuracy without increasing the risk of overfitting. Moreover, this model also demonstrates the ability to learn better representations on large datasets such as Sentinel-1 SAR imagery, making it an ideal choice for flood classification tasks with high accuracy. However, these approaches typically demand high computational resources and rarely integrate ensemble learning methods that could further boost model efficiency and accuracy.

In this context, ensemble learning techniques particularly LightGBM offer a promising solution. LightGBM, a gradient boosting framework, has proven its effectiveness in handling large and high-dimensional datasets, particularly those with imbalanced classes. For instance, a study in China utilized LightGBM for landslide hazard assessment, demonstrating both computational efficiency and strong performance on imbalanced data [25]. When combined with deep learning models like CNN, LightGBM can function as a classifier utilizing the extracted features, improving classification accuracy and training speed. However, such integration remains underexplored in flood classification tasks, despite its potential to enhance both model robustness and efficiency.

This research proposes a novel hybrid approach that integrates CNN for feature extraction and LightGBM for classification. By combining the strengths of both methods, this approach aims to improve classification accuracy, mitigate overfitting, and address class imbalance—all while maintaining computational efficiency. This integration is particularly suited for large and diverse datasets such as SEN12-FLOOD. Unlike prior studies that relied solely on CNN or conventional patch-based methods, this study leverages a synergistic combination of deep learning and ensemble learning. Additionally, it

addresses data imbalance through targeted augmentation techniques and explores the potential of multispectral data integration, offering a more comprehensive and adaptive framework for future flood detection and classification efforts.

3. METHODOLOGY

This methodology outlines the technical steps applied in this research to develop a flood classification model based on Sentinel-1 satellite imagery and machine learning algorithms, specifically Convolutional Neural Networks (CNN) and Light Gradient Boosting Machine (LightGBM). This research aims to improve flood classification accuracy using satellite data processed systematically through several critical stages. As illustrated in Figure 1, the research flow consists of five main stages: data collection, data preprocessing, feature extraction, model training, and model evaluation.

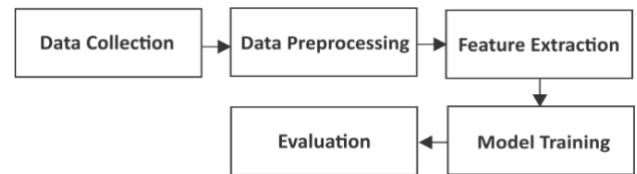


FIGURE 1. RESEARCH METHODOLOGY

3.1 Data Collection

As shown in Figure 1, the first stage of this research is data collection. In this research, the data used for flood classification is radar imagery from Sentinel-1, part of the Copernicus European Space Agency (ESA) program, which provides Synthetic Aperture Radar (SAR) data for monitoring water-related events. SAR imagery is particularly useful under adverse weather conditions, such as heavy rain or thick clouds, which often obstruct optical observations. The dataset used is part of SEN12-FLOOD, which combines Sentinel-1 SAR and Sentinel-2 multispectral data for analyzing flood events. However, this study focuses exclusively on Sentinel-1 data due to its capability to identify water inundation under challenging weather conditions. The Sentinel-1 imagery includes two polarization modes, VV (Vertical-Vertical) and VH (Vertical-Horizontal). VV polarization captures vertical reflections, while VH polarization identifies reflections from inclined surfaces. This complementary information enhances the accuracy of classifying flood and non-flood images.

The spatial resolution of the data is 10 meters, providing sufficient detail for large-scale flood classification. Data collection involves downloading Sentinel-1 imagery from IEEE Data Port, ensuring alignment with the SEN12-FLOOD dataset. All data is pre-labeled as "Flood" or "Non-Flood," simplifying the classification process and allowing the focus to remain on model performance optimization.

3.2 Data Preprocessing

Data preprocessing is a critical stage that prepares SAR imagery for input into machine learning models. It ensures consistency, improves image quality, and addresses challenges such as noise and class imbalance. The

preprocessing steps include image resizing, normalization, noise reduction, data augmentation, and dataset splitting. The overall data preprocessing workflow is illustrated in Figure 2, which outlines the key steps involved in preparing SAR imagery for model training.

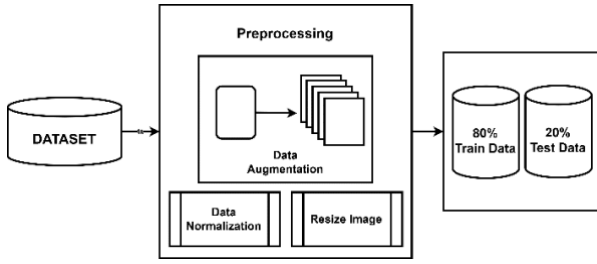


FIGURE 2. DATA PREPROCESSING FLOW

3.2.1 Normalization and Image Resizing

As shown in Figure 2, the preprocessing workflow begins with normalization and image resizing. Image loading is performed using the `scrimmage` library to read and process image files in TIFF format. After loading the images, the first step is resizing. The purpose of resizing is to ensure that all images have consistent dimensions, specifically 128×128 pixels. This step is essential because neural network models, such as CNNs, require inputs with uniform dimensions.

The resizing process is conducted using the `transform.resize()` function, which adjusts image dimensions without significantly altering the aspect ratio or shape of the images. This process also employs interpolation techniques to maintain image quality. Mathematically, resizing using linear interpolation is explained as follows:

$$I'(x', y') = \sum_{(x, y)} I(x, y) \cdot \text{kern}(x' - x, y' - y) \quad (1)$$

In equation (1), $I(x, y)$ represents the intensity of the original pixel, $I'(x', y')$ represents the intensity of the original pixel.

Subsequently, the resized images are normalized. Normalization is performed by dividing pixel values by 255.0, converting the pixel value range from $[0, 255]$ to $[0, 1]$. This normalization aims to reduce scale differences between images, accelerate model training, and improve model convergence.

Mathematically, Min-Max normalization for grayscale images is performed using the following formula:

$$I_{\text{Normalized}} = \frac{I_{\text{Raw}}}{255} \quad (2)$$

In equation (2), I_{Raw} represents the pixel value of the image before normalization, and $I_{\text{Normalized}}$ denotes the pixel value after normalization.

This step helps reduce scale differences between images, accelerates model training, and improves model convergence.

3.2.2 Denoising (Speckle Noise Reduction)

As illustrated in Figure 2, one of the key preprocessing steps is noise reduction to enhance image quality before classification. Synthetic aperture radar (SAR) images often contain speckle noise, a multiplicative noise generated by

the coherent nature of radar signals. This noise can obscure important information in the image and affect the accuracy of machine learning models. Therefore, denoising becomes a crucial step in data preprocessing to enhance image quality.

In this research, denoising is performed using a median filter. The median filter was chosen because of its ability to reduce noise without compromising edges or essential features in the image. This filter works by replacing the value of each pixel with the median value of its neighbors within a defined window.

If $I(x, y)$ is the pixel value at coordinates (x, y) in the original image, then the denoising process with a median filter produces a new pixel value $I_{\text{denoise}}(x, y)$ which is calculated as:

$$I_{\text{denoise}}(x, y) = \text{median}\{I(i, j) : (i, j) \in W(x, y)\} \quad (3)$$

In equation (3), $W(x, y)$ is the filter window that encompasses a square area around the pixel (x, y) , for example, with a size of 3×3 . The median value of the pixels within this window is used to replace the original pixel value at that position.

This process is effective for reducing speckle noise, as the median can ignore extreme values caused by noise without compromising edges or important patterns in the image. The denoising implementation was carried out using the `scipy.ndimage` library with a window size of 3×3 , ensuring that image quality is enhanced before being used for training machine learning models.

3.2.3 Data Augmentation

As shown in Figure 2, data augmentation is applied to enhance dataset diversity and improve model generalization. This process involves various transformations such as rotation, shifting, zooming, and horizontal flipping using the `ImageDataGenerator` library from Keras. Image augmentation is carried out using various random transformations such as rotation, shifting, and horizontal flipping using the `ImageDataGenerator` library from Keras. This process aims to enrich the variety of training images and reduce the risk of overfitting.

Augmentation is performed by considering the class distribution between flood-affected images (Flood) and non-flood-affected images (non-flood). The augmentation factor is set higher for the Flood class since the number of images in this class is smaller than in the non-flood class.

The first transformation applied is rotation, where the image is rotated randomly within the range of $\pm 20^\circ$. Mathematically, this transformation is expressed as:

$$I_{\text{rot}}(x', y') = I(x \cos \theta - y \sin \theta, x \sin \theta + y \cos \theta) \quad (4)$$

In equation (4), x' and y' are the initial coordinates, while x and y are the coordinates after rotation by a random angle θ .

Translation is performed by shifting the image position by up to 20% of the image width (w) or height (h). This transformation is expressed as:

$$I_{\text{trans}}(x', y') = I(x + \Delta x, y + \Delta y) \quad (5)$$

In equation (5), Δx and Δy are random translation values within the range $[-0.2w, 0.2w]$ and $[-0.2h, 0.2h]$,

respectively. Zoom transformation is applied by enlarging or reducing the image size by $\pm 20\%$ of its original size. Mathematically, this zoom transformation is expressed as:

$$I_{\text{zoom}}(x', y') = I(sx, sy) \quad (6)$$

In equation (6), s is a random scaling factor in the range $[0.8, 1.2]$, where $s > 1$ enlarges the image, and $s < 1$ reduces the image size.

Horizontal flipping is used to mirror the image along the horizontal axis, expressed as:

$$I_{\text{flip}}(x', y') = I(w - x, y) \quad (7)$$

In equation (7), w is the width of the image, and flipping is performed by reversing the pixel positions horizontally.

In this study, the augmentation factor is set differently for each class. Images in the Flood class are augmented by a factor of 4, while the non-flood class is augmented by a factor of 2. Additionally, the original images are included in the augmented dataset to retain initial information while enriching the variation in the data.

3.2.4 Dataset Splitting

Following the steps outlined in Figure 2, the final stage of preprocessing is dataset splitting. After augmentation, the dataset is divided into two sets: a training set and a testing set. The split is performed with a ratio of 80% for training data and 20% for testing data. The split is done in a stratified manner, ensuring that the class distribution between Flood and Non-Flood images remains balanced in both sets.

3.3 Feature Extraction

In the feature extraction stage, processed Sentinel-1 radar images are used to identify spatial and textural patterns using a Convolutional Neural Network (CNN) model. CNN is highly effective in detecting texture or surface property changes that are not easily observable, such as those caused by flooding.

In this study, feature extraction is performed using a pre-trained ResNet50 model with local weights, modified specifically for feature extraction. The CNN architecture used is shown in Figure 3.

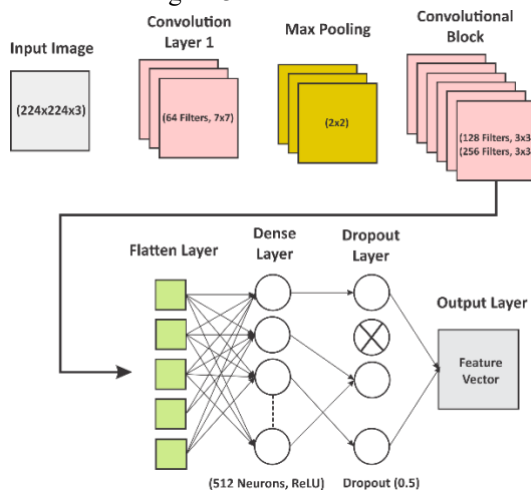


FIGURE 3. CNN ARCHITECTURE

The radar images are preprocessed by resizing them to 224×224 pixels, which is compatible with the ResNet50 model input size. Additionally, since this model is

designed for three-channel (RGB) images, the grayscale Sentinel-1 images are converted to RGB format by replicating pixel intensity values across three channels.

Feature extraction is conducted through convolutional layers to capture local patterns, followed by pooling layers to reduce dimensionality and emphasize the most significant features. This process is visualized in Figure 3, which illustrates the CNN architecture used, including convolution, pooling, and flatten layers that generate feature vectors.

The extracted features are then used as input for the LightGBM classification model, which classifies images into flooded (Flood) and non-flooded (non-flood) categories. The extracted features are stored in CSV format along with their labels, allowing for further analysis without needing re-extraction. By leveraging ResNet50 for feature extraction, this study aims to improve flood classification accuracy using Sentinel-1 SAR imagery.

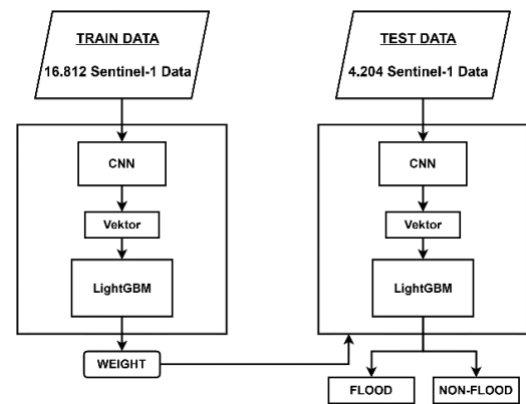


FIGURE 4. EXTRACTION AND CLASSIFICATION FLOW

The feature extraction and classification process in this study begins with training data processed through CNN to generate feature vectors, which are then used to train the LightGBM model. The trained model, with optimized weights, is then used to classify flooded and non-flooded areas on the test data. This process, from feature extraction to final classification, is illustrated in Figure 4.

4. RESULT AND DISCUSSION

The flood classification model developed in this study was trained using a dataset constructed and processed in accordance with the methodology described. The dataset, sourced from Sentinel-1 radar imagery, consisted of 21,016 labeled images divided into two main classes: Flood and Non-Flood. This binary classification task relied on a relatively balanced dataset, with 10,904 Flood images and 10,112 non-flood images. To ensure consistent input dimensions and reduce noise inherent in SAR images, preprocessing steps were applied including resizing, normalization, denoising, and data augmentation. These enhancements aimed to improve data quality and support more effective learning by the model. The dataset was then split into training and testing sets with an 80:20 ratio, resulting in 16,812 images for training and 4,204 for testing.

The model architecture utilized a two-stage approach. In the first stage, feature extraction was performed using the CNN ResNet50 model, which is known for its deep layers and residual connections that allow efficient

learning of spatial and textural patterns from images. This process, applied to all 21,016 images, took approximately 378.11 seconds. After extraction, the data was flattened to shapes of (16,812, 100352) for training and (4,204, 100352) for testing, preparing it for the second stage.

In the second stage, classification was carried out using the LightGBM algorithm. LightGBM was chosen for its high speed and efficiency in handling large-scale data and its capability to deal with class imbalance through built-in optimization techniques. By combining ResNet50's ability to extract rich visual features and LightGBM's fast and accurate classification, the model achieved optimal performance.

The model's performance on the test data is summarized in Table 1, which presents detailed classification metrics.

TABLE 1. METRICS EVALUATION

	Precision	Recall	F1-Score	Support
Non-Flood	0.96	0.95	0.96	2023
Flood	0.96	0.96	0.96	2181
Accuracy			0.96	4204
Macro avg	0.96	0.96	0.96	4204
Weighted avg	0.96	0.96	0.96	4204

These results demonstrate that the model effectively learned from both classes and was able to classify new, unseen test data with high confidence. The equal performance across Precision and Recall indicates that the model does not favor one class over the other, ensuring robust and unbiased predictions. This is particularly important in flood detection tasks, where both false negatives and false positives can have critical consequences in real-world emergency responses.

The model's discriminative ability was further evaluated using the Precision-Recall (PR) curve, as shown in Figure 5. The Area Under the Curve (AUC) value of 0.9852 suggests that the model maintains a strong trade-off between Precision and Recall across all thresholds.

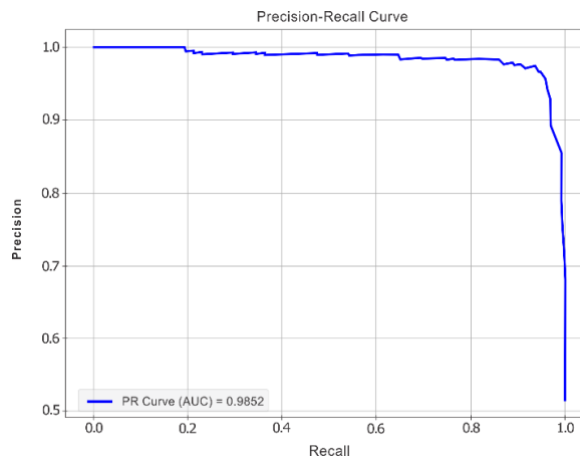


FIGURE 5. PRECISION RECALL CURVE

A high AUC score is essential in flood detection models, as it ensures the model can accurately distinguish between flooded and non-flooded regions. This also confirms the effectiveness of combining ResNet50 for feature extraction with LightGBM for classification.

The classification performance can also be visualized using the confusion matrix presented in Figure 6, which

highlights the correct and incorrect predictions for each class.

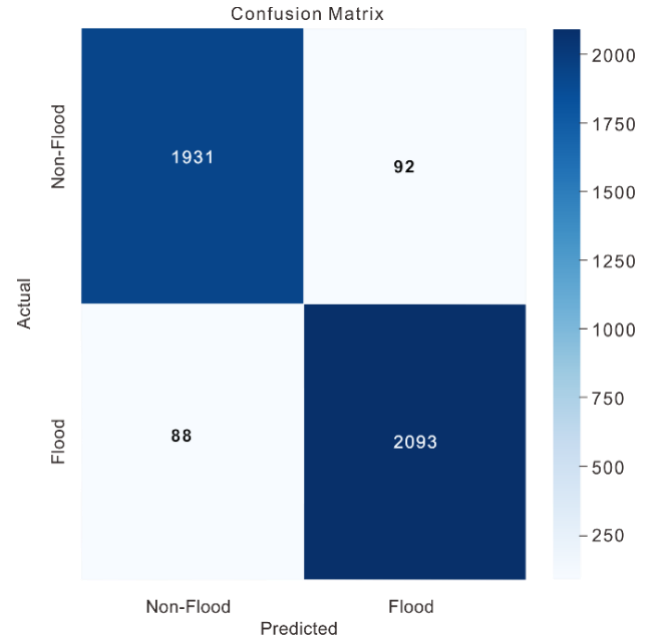


FIGURE 6. CONFUSION MATRIX HEAT MAP

Figure 6, the model correctly identified the majority of flood and non-flood samples, with minimal misclassification. This indicates strong learning capability and reliable generalization across various image characteristics, supporting the model's practical application in real-world satellite-based flood detection systems. These findings underscore the robustness of the model in distinguishing subtle differences in SAR imagery, even under complex environmental conditions.

Furthermore, a detailed evaluation of classification accuracy per class is presented in Table 2, which further supports the reliability of the model.

TABLE 2. CLASSIFICATION PERFORMANCE

Class	Accuracy	Loss
Non-Flood	0.96	0.04
Flood	0.96	0.04

The results in Table 2 indicate that the model consistently classifies both flood and non-flood classes with minimal error. The balanced classification performance is crucial for ensuring practical applicability in real-world flood detection scenarios. This high level of accuracy is essential for early warning systems, where timely and precise flood classification can save lives and reduce economic losses.

Furthermore, the progression of accuracy and loss during model training can be observed in Figure 7 and Figure 8, showing a stable upward trend until the model reaches convergence. The loss graph shows a consistent decline, reflecting effective model learning. The gradual reduction in loss values during training demonstrates that the model successfully minimizes prediction errors over multiple iterations, making it more robust against unseen data. This consistent performance across training epochs indicates that the learning rate and chosen optimization algorithm were well-tuned, contributing to a reliable and generalizable model for practical deployment.

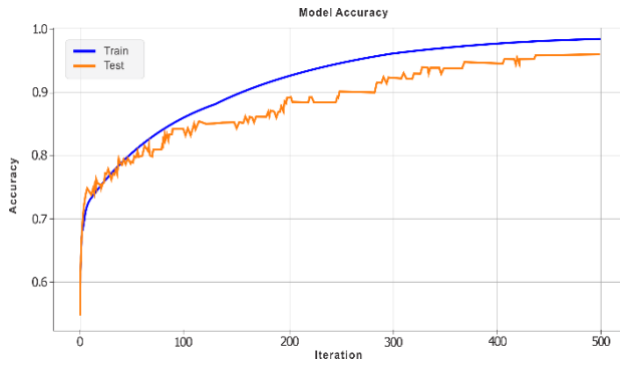


FIGURE 7. ACCURACY MODEL

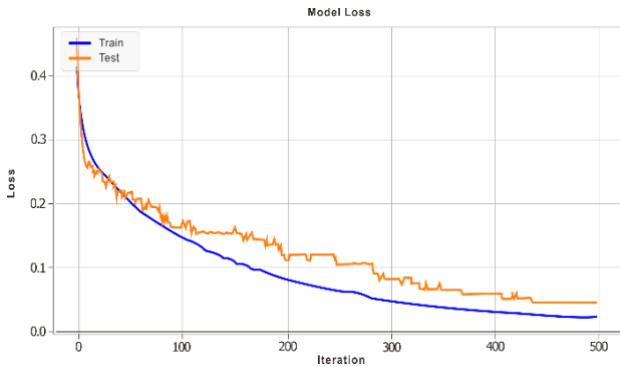


FIGURE 8. LOSS MODEL

In Figure 7, the model accuracy graph shows a stable upward trend during the training process. The model achieved an accuracy of 0.9816 on the training data and 0.9569 on the testing data. This consistent improvement in accuracy reflects the model's ability to effectively learn patterns from the training data. The high accuracy on the testing data also demonstrates the model's capability to generalize effectively, meaning it can perform well on unseen data.

Meanwhile, in Figure 8, the model loss graph indicates a consistent reduction in error throughout the training process. The final loss value reached 0.0184 for the training data and 0.0440 for the testing data. This decline signifies the model's ability to gradually minimize prediction errors as training iterations increase. The small difference between the training loss and testing loss indicates no significant signs of overfitting, ensuring a balance between the model's learning capability on the training data and its generalization on the testing data.

Overall, Figures 7 and 8 illustrate the model's optimal performance during training. The high accuracy and low loss indicate that the combined CNN-ResNet50 approach for feature extraction and LightGBM for classification can work effectively on the Sentinel-1 dataset used. With these results, the model not only demonstrates its ability to learn data patterns well but also shows high reliability when tested on new data. This is crucial to ensure that the model can be implemented in real-world applications, such as satellite radar image-based flood detection systems.

This research also conducted a comparison with previous studies to evaluate the contributions and advantages of the developed model. As presented in Table 3, the CNN-ResNet50 and LightGBM-based approach showed higher accuracy compared to several prior methods.

TABLE 3. COMPARISON OF ACCURACY WITH PREVIOUS RESEARCH

Research Method	Accuracy (%)
SAR-FloodNet	94%
ResNet50-LightGBM (proposed method)	96%

Based on Table 3 previous research utilizing a CNN with the SAR-FloodNet model achieved an accuracy of 94%. In this study, the CNN ResNet50 model was employed for feature extraction, followed by LightGBM for final classification, achieving an improved accuracy of 96% with a final classification time of 55.35 seconds. This increase in accuracy reflects the advantages of the combined CNN-ResNet50 method for feature extraction and LightGBM for classification. The difference in methodology provides added value to the use of ResNet50, which is deeper and capable of capturing spatial and textural features more effectively than standard CNNs. LightGBM also offers benefits in computational efficiency, enabling the model to process data more quickly and handle large datasets more effectively. However, several limitations need to be noted. This study relies solely on Sentinel-1 data, without considering integration with multispectral data from Sentinel-2, which could provide additional information relevant to flood detection. Furthermore, further validation in more diverse environmental conditions is required to ensure the model's reliability across various scenarios.

Overall, this model holds significant potential for application in satellite radar image-based flood detection systems, particularly for classifying flooded and non-flooded areas. Future research integrating multispectral data and testing the model in various environmental conditions could enhance its reliability and expand its applicability.

5. CONCLUSIONS

This research successfully developed a flood classification model based on the combination of CNN-ResNet50 and LightGBM using Sentinel-1 radar imagery. The model demonstrated excellent performance with an accuracy of 96% and high Precision, Recall, and F1-score exceeding 95% for both classes (Flood and Non-Flood). Evaluation results indicate that the model maintains balanced performance across both classes, with good generalization capability on testing data. Additionally, the combination of CNN-ResNet50 for feature extraction and LightGBM for classification has proven to enhance computational efficiency while improving classification accuracy. The key advantage of this model lies in the effective integration of deep feature extraction through CNN-ResNet50 and efficient classification using LightGBM. CNN-ResNet50 can capture detailed spatial and textural features from SAR imagery, while LightGBM enhances classification efficiency, particularly in handling high-dimensional and imbalanced datasets. Compared to previous methods such as SAR-FloodNet, the proposed model improved classification accuracy by approximately 2%, with a final classification time of 55.35 seconds, demonstrating both improved accuracy and reduced computational complexity.

However, there are some limitations to consider, including the exclusive use of Sentinel-1 data without

integration of multispectral data and the need for further validation under diverse environmental conditions. Future studies could involve integrating Sentinel-2 data and testing the model across broader geographic regions to improve reliability and scalability. The application of transfer learning with more optimal parameterization can also be explored to improve accuracy without significantly increasing complexity. In addition, a hybrid approach combining radar and optical data has the potential to provide a more thorough flood analysis, including the detection of impacts to vegetation and infrastructure. With the results obtained, this model has great potential for implementation in flood detection systems based on satellite radar imagery. In addition to contributing to disaster risk mitigation, the model can be integrated into early warning systems to support fast and accurate decision-making in flood-prone areas.

REFERENCES

- [1] P. Ghorpade *et al.*, "Flood Forecasting Using Machine Learning: A Review," *2021 8th International Conference on Smart Computing and Communications: Artificial Intelligence, AI Driven Applications for a Smart World, ICSCC 2021*, pp. 32–36, 2021, doi: 10.1109/ICSCC51209.2021.9528099.
- [2] S. Li, M. Goldberg, S. Helfrich, S. Kalluri, W. Sjoberg, and D. Sun, "Time-Series Global Flood Mapping Datasets from Suomi-NPP&NOAA-20/VIIRS for Flood Analysis and Modelling," *International Geoscience and Remote Sensing Symposium (IGARSS)*, vol. 2023-July, pp. 1004–1007, 2023, doi: 10.1109/IGARSS52108.2023.10283346.
- [3] E. Portales-Julia, N. I. Bountos, M. Sdraka, G. Mateo-Garcia, I. Papoutsis, and L. Gomez-Chova, "Multimodal and Multitemporal Data Fusion for Flood Extent Segmentation Exploiting Kurosiwo and WorldFloods Sentinel Datasets," *International Geoscience and Remote Sensing Symposium (IGARSS)*, pp. 950–953, 2024, doi: 10.1109/IGARSS53475.2024.10690461.
- [4] M. Glasscoe *et al.*, "Integrating Hydrologic Models and Earth Observation Data for Global Flood Forecasting and Alerting in Near Real-Time," *International Geoscience and Remote Sensing Symposium (IGARSS)*, pp. 554–557, 2021, doi: 10.1109/IGARSS47720.2021.9554638.
- [5] B. Demissie, S. Vanhuyse, T. Grippa, C. Flasse, and E. Wolff, "Using Sentinel-1 and Google Earth Engine cloud computing for detecting historical flood hazards in tropical urban regions: a case of Dar es Salaam," *Geomatics, Natural Hazards and Risk*, vol. 14, no. 1, p., 2023, doi: 10.1080/19475705.2023.2202296.
- [6] B. M. Sukojo, L. Azizah, and H. Sanjaya, "Flood Disaster Monitoring Application In The National Rice Granary Area Based On Sentinel-1 Imagery (Case Study: Laren District, Lamongan Regency)," *2023 IEEE International Conference on Aerospace Electronics and Remote Sensing Technology, ICARES 2023*, pp. 1–7, 2023, doi: 10.1109/ICARES60489.2023.10329903.
- [7] M. Nhangumbe, A. Nascetti, and Y. Ban, "Multi-Temporal Sentinel-1 SAR and Sentinel-2 MSI Data for Flood Mapping and Damage Assessment in Mozambique," *ISPRS Int J Geoinf*, vol. 12, no. 2, 2023, doi: 10.3390/ijgi12020053.
- [8] L. J. L. Canillo and A. A. Hernandez, "Flood Risk Visualization and Prediction Information System: Case of City Manila, Philippines," *Proceeding - 2021 IEEE 17th International Colloquium on Signal Processing and Its Applications, CSPA 2021*, no. March, pp. 59–63, 2021, doi: 10.1109/CSPA52141.2021.9377276.
- [9] B. Swapna, R. Venkatesan, F. Taskeen, K. Indrapriya, D. Manjula, and D. S. Muthukumar, "Scalable Deep Learning for Categorization of Satellite Images," *7th International Conference on I-SMAC (IoT in Social, Mobile, Analytics and Cloud), I-SMAC 2023 - Proceedings*, pp. 773–778, 2023, doi: 10.1109/I-SMAC58438.2023.10290437.
- [10] L. Ma, Y. Liu, X. Zhang, Y. Ye, G. Yin, and B. A. Johnson, "Deep learning in remote sensing applications: A meta-analysis and review," *ISPRS Journal of Photogrammetry and Remote Sensing*, vol. 152, no. March, pp. 166–177, 2019, doi: 10.1016/j.isprsjprs.2019.04.015.
- [11] D. Chakravarty, A. M. Thomas, and V. Vivek, "A Survey on Decentralization and Virtualization of Medical Trials: An approach through Ensemble learning models and Convolutional Neural Networks," *2023 International Conference on Computer Science and Emerging Technologies, CSET 2023*, pp. 1–7, 2023, doi: 10.1109/CSET58993.2023.10346978.
- [12] M. Doostparast, M. Pouyani, and M. H. Y. Moghaddam, "Bootstrap Aggregating as an ensemble machine learning algorithm for power consumption prediction under asymmetric loss with linear model-base learners," *2023 27th International Electrical Power Distribution Conference, EPDC 2023*, vol. 0, no. 6, pp. 6–11, 2023, doi: 10.1109/EPDC59105.2023.10218875.
- [13] M. M. Santoni, T. Basaruddin, K. Junus, and O. Lawanto, "Automatic Detection of Students' Engagement During Online Learning: A Bagging Ensemble Deep Learning Approach," *IEEE Access*, vol. 12, no. July, pp. 96063–96073, 2024, doi: 10.1109/ACCESS.2024.3425820.
- [14] R. K. Priyadarshini, A. Bazila Banu, and T. Nagamani, "Gradient Boosted Decision Tree based Classification for Recognizing Human Behavior," *Proceedings of the 2019 International Conference on Advances in Computing and Communication Engineering, ICACCE 2019*, pp. 19–22, 2019, doi: 10.1109/ICACCE46606.2019.9080014.
- [15] C. Arunkumar Madhuvappam, D. Vinod Kumar, S. Kanna, S. Vaishnodevi, G. Murali, and M. Karthick, "Enhanced Lung Cancer Detection using Ensemble Learning Algorithms: A Comparative Study of LightGBM & CatBoost," pp. 324–328, 2024, doi: 10.1109/icipen63822.2024.00060.
- [16] M. R. Machado, S. Karray, and I. T. De Sousa, "LightGBM: An effective decision tree gradient boosting method to predict customer loyalty in the finance industry," *14th International Conference on Computer Science and Education, ICCSE 2019*, no.

- Nips, pp. 1111–1116, 2019, doi: 10.1109/ICCCSE.2019.8845529.
- [17] A. Aparna, A. Emily Jenifer, and N. Sudha, “SAR-FloodNet: A Patch-based Convolutional Neural Network for Flood Detection on SAR Images,” *Proceedings - International Conference on Applied Artificial Intelligence and Computing, ICAAIC 2022*, no. Icaaic, pp. 195–200, 2022, doi: 10.1109/ICAAIC53929.2022.9792770.
- [18] A. Toma, I. Şandric, and B. A. Mihai, “Flooded area detection and mapping from Sentinel-1 imagery. Complementary approaches and comparative performance evaluation,” *Eur J Remote Sens*, vol. 57, no. 1, 2024, doi: 10.1080/22797254.2024.2414004.
- [19] Z. Zhao, B. Zhang, F. Wu, and J. Yang, “Deep Learning-Based Flood Detection Using Multi-Temporal Sentinel-1 SAR Data: A Case Study in Beijing Area, 2023,” *2023 SAR in Big Data Era, BIGSAR DATA 2023 - Proceedings*, pp. 1–4, 2023, doi: 10.1109/BIGSAR DATA59007.2023.10295008.
- [20] C. Singha, V. K. Rana, Q. B. Pham, D. C. Nguyen, and E. Łupikasza, “Integrating machine learning and geospatial data analysis for comprehensive flood hazard assessment,” *Environmental Science and Pollution Research*, vol. 31, no. 35, pp. 48497–48522, 2024, doi: 10.1007/s11356-024-34286-7.
- [21] R. M. A. Latif and J. He, “Flood Susceptibility Mapping in Punjab, Pakistan: A Hybrid Approach Integrating Remote Sensing and Analytical Hierarchy Process,” *Atmosphere (Basel)*, vol. 16, no. 1, pp. 1–32, 2025, doi: 10.3390/atmos16010022.
- [22] H. G. Dong Ye, Qing Xu, “An Efficient and Lightweight Convolutional Neural for Remote Sensing Image Scene Classification,” *S*, 2020.
- [23] C. Qi, Z. Yang, and Y. Wen, “Improved ResNet-50 Model for AI Image Recognition Based on Multi-Scale Attention Mechanism,” *2024 6th International Conference on Communications, Information System and Computer Engineering (CISCE)*, pp. 825–829, 2024, doi: 10.1109/cisce62493.2024.10653161.
- [24] M. Priyanka, S. Sreekumar, and S. Arsh, “Detection of Covid-19 from the Chest X-Ray Images: A Comparison Study between CNN and Resnet-50,” *MysuruCon 2022 - 2022 IEEE 2nd Mysore Sub Section International Conference*, pp. 1–7, 2022, doi: 10.1109/MysuruCon55714.2022.9972488.
- [25] Y. Wang, Y. Ling, T. O. Chan, and J. Awange, “High-resolution earthquake-induced landslide hazard assessment in Southwest China through frequency ratio analysis and LightGBM,” *International Journal of Applied Earth Observation and Geoinformation*, vol. 131, no. June, p. 103947, 2024, doi: 10.1016/j.jag.2024.103947.

AUTHORS



Siddiq Ahmad Anshori

Siddiq Ahmad Anshori is a student of the Informatics program at Universitas Jenderal Achmad Yani (Unjani). His research interests include the application of machine learning and satellite imagery for disaster management, particularly in flood detection.



Asep Id Hadiana

Asep Id Hadiana, S.Si., M.Kom., Ph.D. is an Assistant Professor and researcher in the Informatics Department, Universitas Jenderal Achmad Yani (Unjani). He is both a lecturer and a researcher with a focus on disaster management. His research interests include the prediction and mitigation of natural disasters, particularly around flood prediction. He has been actively involved in several research projects aimed at developing advanced methodologies for disaster risk assessment and management, utilizing state-of-the-art technologies such as remote sensing, machine learning, and geographic information systems (GIS). His work contributes significantly to enhancing disaster preparedness and resilience in vulnerable communities.



Fatan Kasyidi

Fatan Kasyidi, S.Kom., M.T. is a lecturer at the Department of Informatics, Universitas Jenderal Achmad Yani (Unjani). His research interests include machine learning, natural language processing (NLP), affective computing, and speech emotion recognition. He has contributed to several projects related to the integration of machine learning techniques in human-computer interaction and emotional recognition systems.